

---

1 **TECHNICAL NOTE**

2 **Manuscript title:** Effect of infilled materials and arrangements on shear characteristics of  
3 stacked soilbags

4 **Authors:** Kewei Fan<sup>1,2</sup>, Sihong Liu<sup>1</sup>, Yi Pik (Helen) Cheng<sup>2</sup> and Jie Liao<sup>1</sup>

5 **Affiliation:** <sup>1</sup>College of Water Conservancy and Hydropower, Hohai University, Nanjing 210098,  
6 China; <sup>2</sup> Civil, Environmental and Geomatic Engineering, University College London, London WC1E  
7 6BT, UK

8 **Corresponding author:** Sihong Liu, College of Water Conservancy and Hydropower, Hohai  
9 University, Nanjing 210098, China

10 **E-mail:** [sihongliu@outlook.com](mailto:sihongliu@outlook.com)

11 **Abstract**

12 The Shear characteristics of stacked soilbags are related to their interlayer arrangements and  
13 properties of the materials with which the bags(geosynthetics) are filled. To study the effects  
14 of those factors on the shear strength and failure mode of stacked soilbags, a series of shear  
15 tests were conducted. The results show that although the shear failure surface occurred at the  
16 horizontal interface between soilbags when they were arranged vertically, it was ladder-like  
17 when the soilbags were arranged in a staggered manner. The angle of insertion was found to  
18 govern the shape of the shear failure surface, and, thus, the final shear strength of soilbags  
19 arranged in a staggered manner. Two shear failure modes of the stacked soilbags were  
20 observed with different infilled materials. When the frictional resistance of the contact  
21 interface was smaller than the shear strength of the materials with which the bags had been  
22 filled, only interlayer sliding failure occurred. Otherwise, the simple shear failure of materials  
23 filling the bags occurred first, followed by interlayer sliding failure.

24 **Keywords:** Geosynthetics; Soilbag; Contact interface; Shear failure model; Shear strength

---

## 25 1 INTRODUCTION

26 Soilbags or, more precisely, geotextile bags filled with soils or soil-like materials  
27 have high compressive strength (Cheng et al. 2016; Li et al. 2013; Liu et al. 2012).  
28 For example, an ordinary polypropylene (PE) bag filled with crushed stones or sand  
29 (approximately 40cm × 40cm × 10cm) can withstand a load of up to 230~280 kN.  
30 Therefore, the soilbag is also known as ‘soft stone’. Matsuoka and Liu (2003) found  
31 that the high compressive strength of soilbags can be theoretically explained by the  
32 increased apparent cohesion that develops due to the tensile force of the wrapped bag  
33 under external loading, they developed, therefore, soilbags into a new way to  
34 reinforce the foundation of the building. Soilbags have thus far been used to reinforce  
35 hundreds of the foundations in Japan and China (Ding et al. 2018; Liu et al. 2014; Liu,  
36 2017; Matsuoka and Liu, 2014; Xu et al. 2008), They have many advantages such as  
37 low cost, environmental friendliness, reduced traffic-induced vibration, and the  
38 prevention of frost heave.

39 The use of soilbags has recently been extended to earth-retaining structures, such  
40 as retaining walls (Liu et al. 2019; Portelinha et al. 2014; Wang et al. 2015) and slopes  
41 (Liu et al. 2012, 2015; Wang et al. 2019). Many researchers have claimed that the  
42 stability of earth-retaining structures constructed using soilbags is closely related to  
43 their interlayer friction, on which considerable research has been conducted using  
44 shear tests (Ansari et al. 2011; Basudhar, 2010; Krahn et al. 2007; Liu et al. 2016.,  
45 Lohani et al. 2006; Matsushima et al. 2008). The relevant studies accumulated a vast  
46 amount of data on the interlayer friction in engineering structures built using soilbags.  
47 However, the only interlayer sliding failure mode, a horizontal line on the plane, is  
48 considered when stacked soilbags are subjected to shear forces, and interlayer  
49 frictional resistance between vertically stacked soilbags is treated as their shear  
50 strength. However, Fan et al. (2019) found that the sliding surface in a  
51 model-retaining wall stacked in a staggered manner is ladder-like due to the insertion  
52 of soilbags. The soilbag is a composite of woven bags and the materials filling them.  
53 The shear strength and deformation of soilbags may be related not only to the

---

54 interlayer friction of woven bags, but also to the mechanical properties of the  
55 materials with which they are filled, where those vary for pure sand and  
56 coarse-grained soil (pebbles).

57 In this paper, a series of shear tests on soilbags, packed with two materials of  
58 different grain sizes, and stacked up in two interlayer arrangements, are conducted to  
59 study the effect of materials filling the bags and the interlayer arrangements on the  
60 shear strength and failure mode of the stacked soilbags.

## 61 **2 TESTING SCHEMES AND MATERIALS**

62 Soilbags are usually arranged either vertically or in a staggered manner in  
63 engineering practice, and are filled with soils excavated from the field. Different  
64 arrangements and grain sizes of the materials with which soilbags are filled can lead  
65 to different contact interfaces. Fig. 1(a) shows a flat contact interface of vertically  
66 arranged soilbags with fine-grain fill (sand), while Fig1(b) shows an uneven contact  
67 interface of vertically arranged soilbags with coarse-grain fill (pebble). The effect of  
68 the uneven contact interface is defined as ‘interlock’ in this paper. Fig. 1(c) shows  
69 stacked soilbags arranged in a staggered manner. Due to their flexibility, soilbags in  
70 the upper layer can deform into gaps between those in the lower layer with embedded  
71 contact when subjected to vertical load. This is defined as ‘insertion’ in this paper. To  
72 study the shear characteristics of stacked soilbags with materials of different grain  
73 sizes filling them and the interlayer arrangements, four shear tests were designed  
74 (Table 1). Three layers of sand-filled soilbags, or those filled pebbles, were vertically  
75 arranged to observe the deformation in the stacked soilbags more clearly.

76 Soilbags of size 40cm × 40cm × 10cm, which are typically used in engineering  
77 practice (Liu et al., 2015; Matsuoka and Liu, 2003; Xu et al., 2008), were used in the  
78 shear tests. The woven bags were made of polypropylene and weighted 150g/m<sup>2</sup>, and  
79 the coefficient of friction of the two sheets of the bags was 0.34. To prevent the woven  
80 bags from being scratched by pebble particles, most of the filled pebbles were nearly  
81 elliptical in shape. Moreover, the surface of the pebbles was very smooth. The  
82 physical and mechanical properties of the infilled sand and pebbles are listed in Table

---

83 2. The initial densities of the sand and pebbles inside the woven bags were  $1.63\text{g/cm}^2$   
84 and  $1.68\text{ g/cm}^2$ , respectively.

### 85 **3 TESTING APPARATUS**

86 A direct shear test apparatus was designed to test the shear characteristics of the  
87 stacked soilbags, as shown in Fig. 2. The samples of the stacked soilbags were placed  
88 on a steel base plate so that their bottom layers could be fixed onto the base plate by  
89 two angle plates made of steel. A rigid, rough metal loading plate with two side plates  
90 was placed on top of the sample. The soilbag in the top layer was sandwiched  
91 between the side plates so that they could move with the loading plate. A displacement  
92 transducer was fixed onto the side plate to monitor horizontal displacement. The left  
93 end of the loading plate was connected to a horizontal tension device. The height of  
94 the tension device could be adjusted with the height of the sample by rotating the  
95 screw caps on the screw stems. A horizontal tension force was applied at a speed of 2  
96 mm/min by a screw rotation axel, and a load cell was fixed to the left of the tension  
97 device to monitor the horizontal force. Vertical loads were applied to the loading plate  
98 by a motor. Some ball bearings were set between the loading plate and the vertical  
99 loading device to reduce the friction between them. Several (red) marker lines, as  
100 shown in Fig. 2, were placed on the soilbags and the metal loading plate to obtain the  
101 deformation and slip surface of the soilbags by measuring the relative displacement of  
102 the marker lines. The spacing between vertical lines was 10cm. Finally, a camera was  
103 positioned in front of the setup of the shear tests to monitor the movement of the  
104 markers at regular intervals.

### 105 **4 TEST RESULTS**

#### 106 **4.1 Solibags filled with sand**

107 Fig. 3 shows the horizontal shear stress plotted against shear displacement in  
108 tests T1S and T2S when the applied normal stress is at  $\sigma_n = 80\text{kPa}$ . The development  
109 of the stress-displacement curve can be divided into two stages for T1S and three  
110 stages for T2S. The shear stress increased with the shear displacement in the first  
111 stage OA, which was similar in both T1S and T2S. Although test T2S featured slightly

---

112 higher shear stress in the first stage, the impact was minimal. In this stage, the end of  
113 the soilbag at which force was applied was first locally compressed by the shear force  
114 due to the flexibility of the soilbag filled with sand. This can be verified by the  
115 phenomenon shown in Fig. 4, where the marker lines on the metal loading plate move  
116 away from those on soilbags in the top layer. When the shear stress reached the  
117 maximum shear resistance of the contact interface between the soilbags, that in top  
118 layer slid relative to soilbag in the middle-layer soilbag (see Fig. 4). In stage AB of  
119 test T1S, the shear stress remained constant. For test T2S, the soilbag in top layer  
120 deformed to settle into the gap between soilbags (insertion) in the lower layer owing  
121 to the vertical load and the flexibility of the soilbags. This insertion prevented the  
122 upper soilbag from sliding immediately at point A in T2S. During stage AC, the end of  
123 the soilbag was further compressed. However, there was an additional increase in  
124 shear stress (Stage AC) before it reached the maximum shear strength in test T2S.  
125 Additional horizontal stress was to be mobilized due to the inclined angles of the  
126 soilbag interface, reducing the efficiency of the interface friction. This is verified  
127 further in Fig. 7 and Eq. (5) below. Finally, the shear stress reached the maximum  
128 shear strength and soilbag in the top layer began to slide as a whole at point C.

129 Fig. 5 presents the relationship between the final shear stress and normal stress in  
130 the tests T1S and T2S. It is clear that the final stress in T2S was greater than that in  
131 T1S under the same normal stress due to insertion. The calculated shear stress,  $\tau$ ,  
132 versus normal stress,  $\sigma_n$ , of the woven bags based on the friction angle,  $\phi_{\text{bag}}$ , is also  
133 shown in Fig. 5, from which it is clear that the peak shear strength of the sand-filled  
134 soilbags was only slightly larger than that of the woven bags. This is because the sand  
135 particles were relatively small in size such that some poured out of the woven bags,  
136 and became trapped in the contact interface between soilbags. These sand particles  
137 slightly increased the sliding resistance. The curve of the peak shear strength for test  
138 T2S was always higher than that for T1S due to the mechanism explained earlier in  
139 section 4.1, and was not straight. This was related to the measured angle of insertion  
140 shown in Fig. 6. It increased as normal stress increased. To quantify the relationship

141 between the shear force and the angle of insertion, the force acting on the upper  
142 soilbag in test T2S was analyzed using the data shown in Fig. 7.

143 If it is assumed that the contact interface between the soilbags was composed of  
144 two inclined surfaces at the same angle of inclination,  $\theta$ , the height,  $H$ , and length,  $B$ ,  
145 of the soilbag were assumed to be unchanged under normal stress. The forces acting  
146 on the soilbag consist of the normal stress,  $\sigma$  (normal stress produced by deadweight  
147 of the soilbags was calculated together with stress,  $\sigma$ ), the reactions at the bottom of  
148 the soilbags  $N_1$  and  $N_2$ , corresponding friction,  $f_1$  ( $f_1=\mu N_1$ ), and  $f_2$  ( $f_2=\mu N_2$ ), and the  
149 shear force,  $F_{T2S}$ . The coefficient of interface friction of two vertically stacked  
150 soilbags filled with sand is given by  $\mu$ . Using the equations of the equilibria of force  
151 and moment about point O, the following can be obtained

$$152 \quad \sum F_x = 0: (N_1 - N_2) \sin \theta + (N_1 + N_2) \mu \cos \theta = F_{T2S} \quad (1)$$

$$153 \quad \sum F_y = 0: (N_1 + N_2) \cos \theta - (N_1 - N_2) \mu \sin \theta = \sigma B \quad (2)$$

$$154 \quad \sum M = 0: (N_1 + N_2) \mu B / 2 \sin \theta + (N_2 - N_1) B / 4 [1 - 2 \sin^2 \theta] / \cos \theta + 1/2 F_{T2S} H = 0 \quad (3)$$

155 Solving for  $F_{T2S}$ ,

$$156 \quad F_{T2S} = \beta \mu \sigma B = \beta F_{T1S} \quad (4)$$

$$157 \quad \text{where,} \quad \beta = \frac{B}{-B + 2B(1 + \mu^2) \sin^2 \theta + H(1 + \mu^2) \sin 2\theta} \quad (5)$$

158 From Equation (4) that the shear force,  $F_{T2S}$ , with insertion, compared with the  
159 shear force without insertion  $F_{T1S}$  ( $F_{T1S} = \mu \sigma B$ ), was expanded by  $\beta$  when  $\beta > 1$ .  
160 Hence  $\beta$  was related to the angle of insertion  $\theta$ . The calculated coefficient  $\beta$  versus  
161 normal stress is shown in Fig. 8, from which it is clear that  $\beta$  as calculated from  
162 Equation (5) using the observed insertion  $\theta$  agreed reasonably well with the  
163 experimentally derived  $\beta$ , where  $\beta = (\tau_f / \sigma_n) / \mu$ ,  $\tau_f$  is the measured final shear stress and  $\sigma_n$   
164 is the normal stress. Moreover,  $\beta$  reached a value of up to 1.41 under a normal stress  
165 of 100kPa, which means that insertion can significantly increase the interlayer friction  
166 of the soilbags. This phenomenon is beneficial for the stability of a structure built  
167 using soilbags.

---

168        However, through the shear tests on five layers of soilbags arranged in a  
169 staggered manner under different vertical loads, Fan et al. (2019) found that the  
170 sliding surface in the shear tests was nearly horizontal under small vertical loads, and  
171 ladder-like under large vertical loads, as shown in Fig. 9. The shape of the sliding  
172 surface changed from being a horizontal line to a ladder-like shape because the  
173 insertion of the soilbags increased with the vertical load. Therefore, in case of large  
174 vertical loads, the shear strength should not be calculated using Equation (4) because  
175 the sliding surface changed. Instead, the methods proposed by Fan et al. (2019) should  
176 be used.

#### 177 **4.2 Soilbags filled with pabbles**

178        Fig. 10(a) shows the shear stress versus shear displacement for tests T1P (for  
179 soilbags filled with pebbles) and T1S (for soilbags filled with sand), both of which  
180 featured vertically stacked soilbags. It is clear that the shear stress-displacement  
181 curves in test T1P were not identical to those of T1S. Stage OA was nearly identical  
182 for both tests, implying that the soilbag was initially compressed by the horizontal  
183 shear force. Stage DB in test T1P featured the same mechanism as stage AB in test  
184 T1S, and the soilbag in the top layer slid relative to that in the middle layer (see Fig.  
185 11(b)). However, stage AD in T1P did not exist in T1S due to the deformation of the  
186 soilbag filled with pebbles before they slid, and the mechanism is shown through the  
187 shear stress-strain curve plotted in Fig. 10(b). The rotational shear strain,  $\gamma$ , increased  
188 because the shear stress caused the soilbags to deform into a parallelogram, as shown  
189 in Fig. 11(a). However, no rotational shear strain was observed in test T1S. This is  
190 discussed later in section 5.

191        The shear stresses in the middle, stable part (AC) and the final, stable part (DB)  
192 in T1P are called the intermediate shear stress,  $\tau_{int}$ , and final shear stress,  $\tau_f$ ,  
193 respectively. Fig. 12 plots the final shear stress versus normal stress. It is clear that  
194 the final shear stress was larger than that of the woven bags,  $\tau_{bag}$ , but was smaller  
195 than that of the pebbles,  $\tau_{pebble}$ . This implies that the use of woven bags reduced the

---

196 frictional coefficient of the pebbles, or that the use of pebbles increased the frictional  
197 coefficient of the woven bags.

198 The measured angle of insertion of shear tests on the soilbags filled with pebbles  
199 is plotted in Fig. 6. It is clear from this that the angle of soilbags filled with pebbles  
200 was smaller than that of the soilbags filled with sand. This is because the size of  
201 particles of pebbles was larger than those of sand, which made soilbags filled with  
202 pebbles difficult to deform into gaps between soilbags in the bottom layer. This will  
203 cause  $\beta$  calculated from Equation (5) of soilbags filled with pebbles smaller than that  
204 of soilbags filled with sand under same vertical load, which means that insertion of  
205 soilbags filled with pebbles is smaller compared with that of sand-filled soilbags. Fig.  
206 13 shows the final shear stress versus normal stress for T2S and T2P. It shows that  
207 the final stresses for tests T2S and T2P were significantly larger than those of the  
208 woven bags as a result of insertion and interlock. However, insertion played a  
209 dominant role in influencing the shear strength of stacked soilbags filled with small  
210 and regular shaped particles(sand), whereas interlocking was dominant for stacked  
211 soilbags filled with large and irregularly shaped particles(pebble).

## 212 **5 Discussion**

213 To determine why the soilbags filled with pebbles initially underwent shear  
214 deformation during shearing, whereas the sand-filled soilbags did not, the state of  
215 stress of an element inside the soilbags under normal stress,  $\sigma_n$ , was analyzed. Under  
216 normal stress, the compression deformation of the soil caused the perimeter of the bag  
217 increased, which led to and induced tensile force  $T$  along the bag (Matsuoka and Liu,  
218 2003). In practice, the induced tension may not be uniform along the bag, but was  
219 assumed to be constant here throughout the bag. Fig.14 (a) shows a 2D element of soil  
220 (either sand or pebbles) inside soilbags in the middle layer. The forces acting on this  
221 element consisted of the normal stress  $\sigma_z = \sigma_n + 2T/B$ , lateral stress  $\sigma_x = 2T/H$ , and shear  
222 stress,  $\tau$ , assuming no slip between the woven bag and the materials filling it. A Mohr  
223 circle for the element was drawn, as shown in Fig.14 (b). With increasing shear stress  
224 during shearing, the radius of the Mohr circle increased. When the Mohr circle

225 touched the Coulomb failure line of the materials filling the soilbags, the materials  
 226 reached failure with large deformation. The shear stress that caused them to deform is  
 227 defined as the critical shear stress,  $\tau_{crit}$  and can be expressed as,

$$228 \quad \tau_{crit} = \frac{1}{2} \sqrt{(\sigma_z + \sigma_x)^2 \sin^2 \phi - (\sigma_z - \sigma_x)^2} \quad (6)$$

229 If the interfacial shear strength,  $\tau_f$ , between soilbags was smaller than that of the  
 230 materials filling them,  $\tau_{crit}$ , only sliding along the interface occurred. Otherwise,  
 231 failure of materials filling the soilbags due to deformation first occurred, followed by  
 232 sliding along the interface.

233 To calculate the value of  $\tau_{crit}$  of soilbags filled with sand and pebbles, the  
 234 mobilized tensile stresses  $T$  of bags under different normal stresses were determined.  
 235 Separate tests were conducted by loading three soilbags stacked vertically to obtain  
 236 the relationship between the tensile strain acting along with the bags and the applied  
 237 normal stress. Before the compression load was applied, four points were marked on  
 238 the front, back, right and left sides of the surface of the soilbags in the middle layer, of  
 239 which two points were marked on the warp strip and two on the weft strip. The initial  
 240 distance between the points was 10cm. A string was attached to the surface to simulate  
 241 the distance between points, and a ruler with an accuracy of 0.1mm was used to  
 242 measure the length of the string. The average value of eight measurements was used  
 243 to calculate the tensile stress, as shown in Fig. 15. Tensile stress  $T$  corresponding to  
 244 each value of tensile strain was then obtained from a simple tension test. A device  
 245 called ‘multi-functional biaxial tensile testing machine’ (Wu et al. 2014) was used to  
 246 test the woven sheet of size 5cm × 10cm. The rate of stretching of the sheet was  
 247 0.25mm/min, and the results are as shown in Fig. 16.

248 Fig. 17 shows all the experimental value of  $\tau_f$  (T1S and T1P) and the calculated  
 249  $\tau_{crit}$  (Equation (6)) of soilbags filled with sand and pebbles. It is clear that the  
 250 calculated critical shear stress of the soilbag filled with pebbles  $\tau_{crit-pebble}$  (calculated)  
 251 using Equation (6) agreed with the measured intermediate shear stress  $\tau_{int-pebble}$  (T1P) in  
 252 the T1P. This means that the intermediate shear stress causing the shear deformation

---

253 of the stacked soilbags filled with pebbles can be measured by the shear test on them.  
254 Fig.17 also shows that for sand-filled soilbags,  $\tau_{f-sand(TIS)} < \tau_{crit-sand (calculated)}$ , which  
255 means that they did not deform before sliding. On the contrary, for soilbags filled  
256 with pebbles,  $\tau_{f-pebble(TIP)} > \tau_{crit-pebble(calculated)} \approx \tau_{int-pebble(TIP)}$ , which means that they  
257 deformed before sliding. Note that in practice, for retaining structures built or  
258 reinforced using soilbags with strict requirements for displacement, the intermediate  
259 shear stress should be regarded as the shear strength rather than the final stress.  
260 Otherwise, the final shear stress can be used for design.

## 261 **6 Conclusion**

262 A series of shear tests were conducted in this study to examine the effects of  
263 materials filling bags and interlayer arrangements on the shear strength and  
264 deformation of the stacked soilbags. Based on the results, the following conclusions  
265 can be obtained:

- 266 (1) The shear strength of soilbags with different arrangements was found to be related  
267 to the shape of the shear failure surface. This surface is the interface between  
268 soilbags when they are arranged vertically, but is ladder-like when arranged in a  
269 staggered manner.
- 270 (2) Two shear failure modes of the stacked soilbags were observed filled with two  
271 materials. When the final shear strength of the interface was smaller than the  
272 critical shear strength of the materials filling the bags, only interlayer sliding  
273 failure occurred. Otherwise, the failure due to deformation of the materials  
274 occurred first, followed by sliding failure.

## 275 **Acknowledgements**

276 This work was supported by the National Key R&D Program of China (Grant No.  
277 2017YFE0128900). It was also part of a project funded by the China Scholarship  
278 Council (No. 201806710071).

---

**279 References**

- 280 Ansari, Y., Merifield, R., Yamamoto, H. & Sheng, D. (2011). Numerical analysis of  
281 soilbags under compression and cyclic shear. *Geotextiles and Geomembranes*, 38:  
282 659-668.
- 283 Basudhar, P. (2010). Modeling of soil–woven geotextile interface behavior from  
284 direct shear test results. *Geotextiles and Geomembranes*, 28: 403-408.
- 285 Cheng, H., Yamamoto, H. & Thoeni, K. (2016). Numerical study on stress states and  
286 fabric anisotropies in soilbags using the DEM. *Computers and Geotechnics*, 76:  
287 170-183.
- 288 Ding, G., Wu, J., Wang, J. & Hu, X. (2017). Effect of sand bags on vibration  
289 reduction in road subgrade. *Soil Dynamics and Earthquake Engineering*, 100:  
290 529-537.
- 291 Fan K., Liu S.H., Cheng Y.P. & Wang Y.S. (2019). Sliding stability analysis of a  
292 retaining wall constructed by soilbags. *Geotechnique Letters*, 9(3): 211-217
- 293 Krahn, T., Blatz, J., Alfaro, M. & Bathurst, R. (2007). Large-scale interface shear  
294 testing of sandbag dyke materials. *Geosynthetics International*, 14: 119-126.
- 295 Li, Z., Liu, S.H., Wang, L. & Zhang, C. (2013). Experimental study on the effect of  
296 frost heave prevention using soilbags. *Cold Regions Science and Technology*, 85:  
297 109-116.
- 298 Liu, S.H., Bai, F., Wang, Y., Wang, S. & Li, Z. (2012). Treatment for expansive soil  
299 channel slope with soilbags. *Journal of Aerospace Engineering*, 26: 657-666.
- 300 Liu, S., Bai, F., Wang, Y., Wang, S., & Li, Z. (2012). Treatment for expansive soil  
301 channel slope with soilbags. *Journal of Aerospace Engineering*, 26(4): 657-666.
- 302 Liu, S.H., Fan, K., Chen, X., Jia, F., Mao, H. & Lin, Y. (2016). Experimental studies  
303 on interface friction characteristics of soilbags. *Chinese Journal of Geotechnical*  
304 *Engineering*, 38: 1874-1880.
- 305 Liu, S.H., Fan, K. & Xu, S. (2019). Field study of a retaining wall constructed with  
306 clay-filled soilbags. *Geotextiles and Geomembranes*, 47: 87-94.
- 307 Liu, S.H., Gao, J.J., Wang, Y.Q., Weng, L.P., 2014. Experimental study on vibration

- 
- 308 reduction by using soilbags. *Geotextiles and Geomembranes* 42, 52-62.
- 309 Liu, S., Lu, Y., Weng, L., & Bai, F. (2015). Field study of treatment for expansive  
310 soil/rock channel slope with soilbags. *Geotextiles and Geomembranes*, 43(4):  
311 283-292.
- 312 Liu, S.H. (2017). *Principle and application of soilbags*. Science Press, Nanjing,  
313 China.
- 314 Lohani, T., Matsushima, K., Aqil, U., Mohri, Y. & Tatsuoka, F. (2006). Evaluating  
315 the strength and deformation characteristics of a soil bag pile from full-scale  
316 laboratory tests. *Geosynthetics International*, 13: 246-264.
- 317 Matsuoka, H. & Liu, S.H. (2003). New earth reinforcement method by soilbags ("  
318 Donow"). *Soils and Foundations*, 43: 173-188.
- 319 Matsuoka, H. & Liu, S.H. (2014). *A new earth reinforcement method using soilbags*.  
320 CRC Press, London, UK.
- 321 Matsushima, K., Aqil, U., Mohri, Y. & Tatsuoka, F.J.G.I. (2008). Shear strength and  
322 deformation characteristics of geosynthetic soil bags stacked horizontal and  
323 inclined. *Geosynthetics International*, 15: 119-135.
- 324 Portelinha, F., Zornberg, J. & Pimentel, V. (2014). Field performance of retaining  
325 walls reinforced with woven and nonwoven geotextiles. *Geosynthetics*  
326 *International*, 21: 270-284.
- 327 Wang, L.J., Liu, S.H., & Zhou, B. (2015). Experimental study on the inclusion of  
328 soilbags in retaining walls constructed in expansive soils. *Geotextiles and*  
329 *Geomembranes*, 43: 89-96.
- 330 Wang, Y. Q., Liu, K., Li, X., Ren, Q. B., Li, L. L., Zhang, Z. H., & Li, M. C. (2019).  
331 Experimental and upper-bound study of the influence of soilbag tail length on the  
332 reinforcement effect in soil slopes. *Geotextiles and Geomembranes*, 103460.
- 333 Wu, H., Su, Y., Cao, M., & Jiang, X. (2014). Development and application of  
334 multi-functional biaxial tensile testing machine for geosynthetics. *Chinese*  
335 *Journal of Geotechnical Engineering*, 36(1): 170-175.
- 336 Xu, Y., Huang, J., Du, Y. & Sun, D.A. (2008). Earth reinforcement using soilbags.



338 **Table Captions**

339 Table 1 Programs of shear tests on soilbags.

340 Table 2 Physical and mechanical parameters of soilbags filled with sand and pebbles

Table 1 Programs of shear tests on soilbags

---

| Test | Materials | Interlayer<br>arrangement | No. of<br>Layers |
|------|-----------|---------------------------|------------------|
| T1S  | Sand      | Vertically                | 3                |
| T2S  | Sand      | Staggered                 | 2                |
| T1P  | Pebbles   | Vertically                | 3                |
| T2P  | Pebbles   | Staggered                 | 2                |

---

342 Table 2 Physical and mechanical parameters of soilbags filled with sand and  
343 pebbles

| Materials          | D <sub>30</sub><br>(mm) | D <sub>50</sub><br>(mm) | D <sub>60</sub><br>(mm) | D <sub>90</sub><br>(mm) | $\rho_{min}$ | $\rho_{max}$ | $c$ | $\phi_{peak}(\circ)$ |
|--------------------|-------------------------|-------------------------|-------------------------|-------------------------|--------------|--------------|-----|----------------------|
| Natural river sand | 0.32                    | 0.36                    | 0.4                     | 0.75                    | 1.43         | 1.77         | 0   | 35.4                 |
| Pebbles            | 21.2                    | 28.7                    | 32.4                    | 45.6                    | 1.62         | 2.01         | 0   | 29.2                 |

---

**Figure Captions**

344  
345 Figure 1. Schematic view of the insertion and interlock of stacked soilbags: in  
346 vertically arranged soilbags filled with (a) fine-grain materials, (b) coarse-grain  
347 material, and (c) soilbags arranged in a staggered manner.

348 Figure 2. Schematic view of the shear test on stacked soilbags.

349 Figure 3. Shear stress versus shear displacement in tests T1S and T2S at  $\sigma_n = 80\text{kPa}$ .

350 Figure 4. Deformation of soilbags during shearing in T1S.

351 Figure 5. Final shear stress versus normal stress in T1S and T2S.

352 Figure 6. Angle of insertion versus normal stress in tests T2S and T2P.

353 Figure 7. Analysis model for T2S.

354 Figure 8. Coefficient  $\beta$  versus normal stress in T2S.

355 Figure 9. Different sliding surfaces in shear tests on five-layer soilbags

356 Figure 10. Shear stress versus shear displacement and shear strain (rotation) in tests  
357 T1S and T1P at  $\sigma_n = 80\text{kPa}$ : (a) Shear stress versus shear displacement and (b) Shear  
358 stress versus shear strain.

359 Figure 11. Status of soilbags filled with pebbles during shearing in T1P: (a)  
360 Deformation of materials filling the bag in T1P and (b) Interlayer sliding failure.

361 Figure 12. Final shear stress versus normal stress in test T1P.

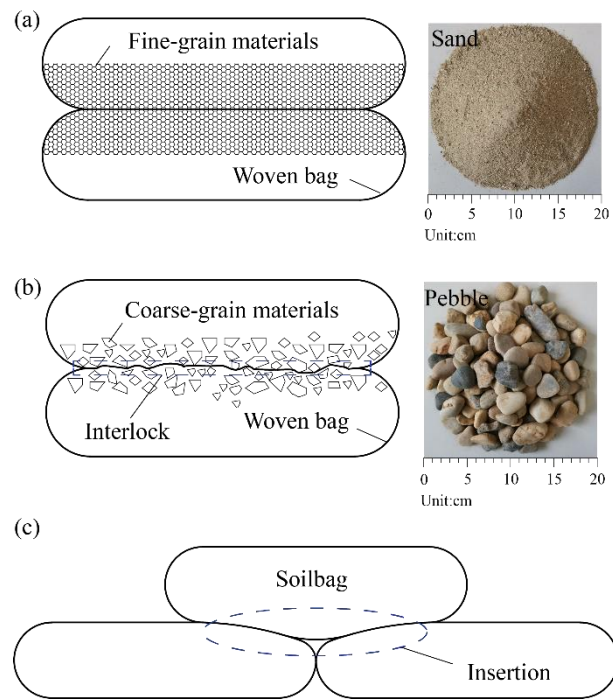
362 Figure 13 Final shear stress versus normal stress in test T2S and T2P

363 Figure 14. Stress analysis of the element inside the soilbags.

364 Figure 15. Tensile strain of woven bag versus normal stress applied on soilbag.

365 Figure 16. Tensile behavior of the woven bags.

366 Figure 17.  $\tau_f$  and  $\tau_{crit}$  versus normal stress of soilbags.



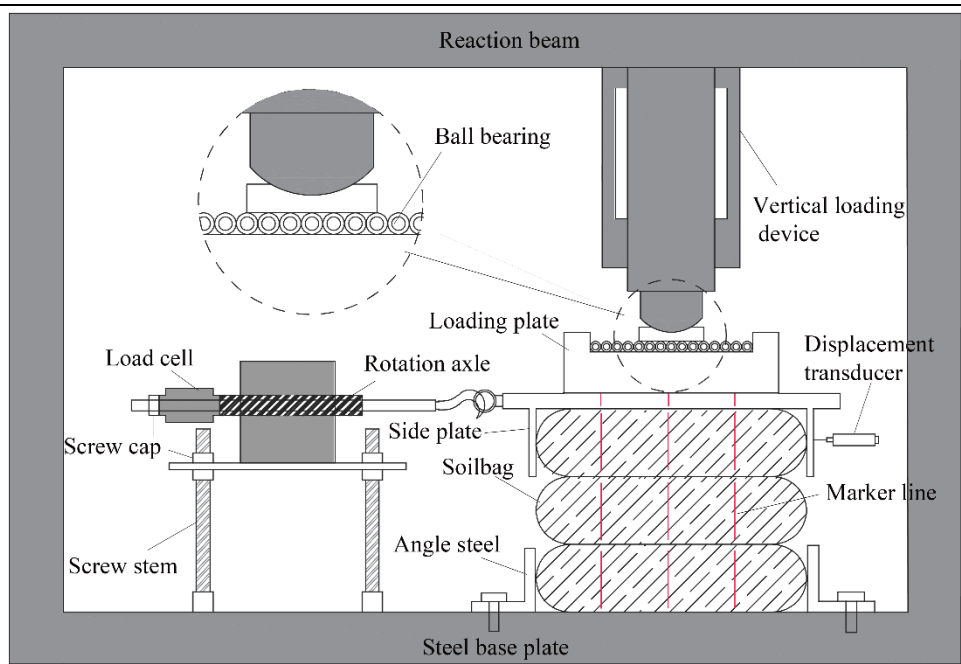
367

368

369

370

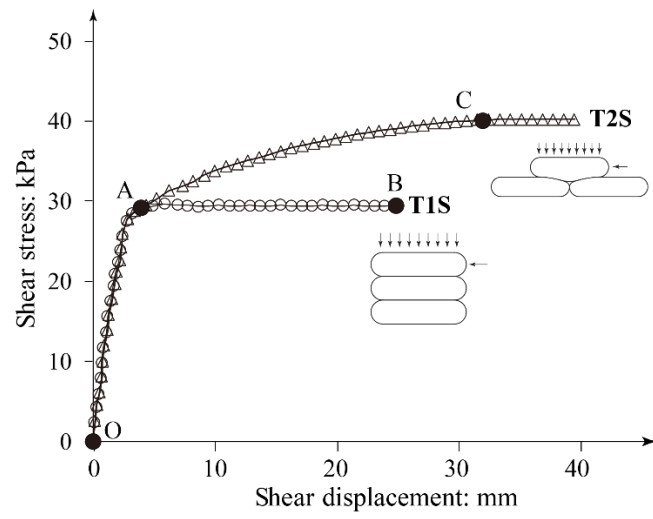
Fig.1 Schematic view of the insertion and interlock of stacked soilbags: in vertically arranged soilbags filled with (a) fine-grain materials, (b) coarse grain material and (c) soilbags arranged in a staggered manner



371

372

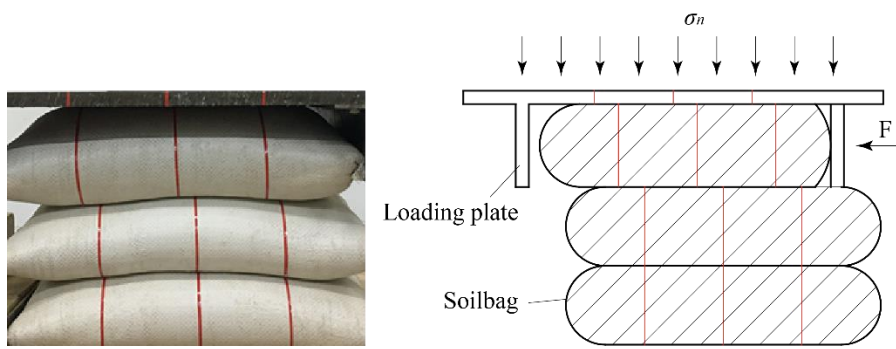
Fig.2 Schematic view of the shear test on stacked soilbags



373

374

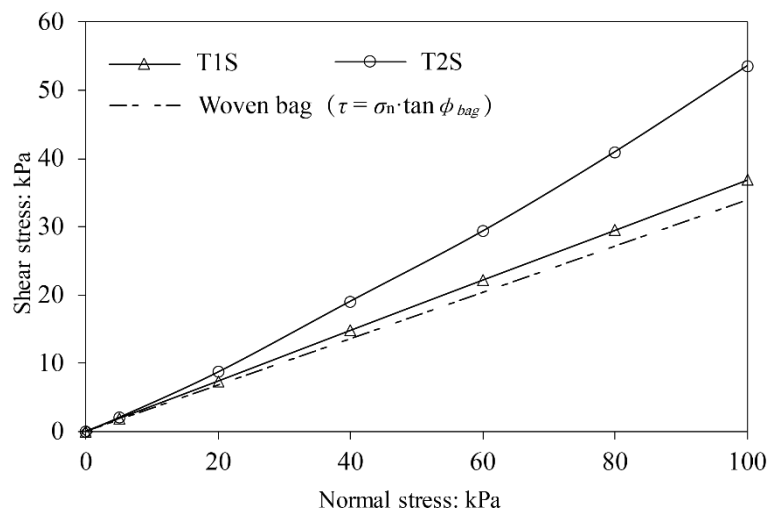
Fig.3 Shear stress versus shear displacement in tests T1S and T2S at  $\sigma_n = 80\text{kPa}$



375

376

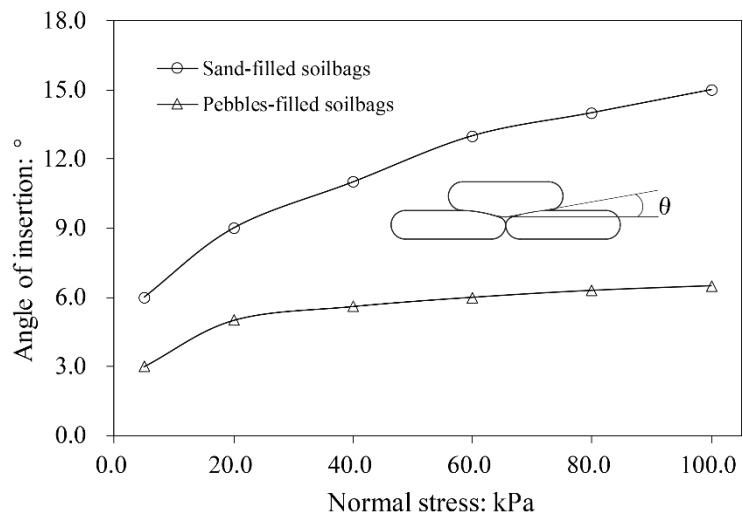
Fig.4 Deformation of soilbags during shearing in T1S



377

378

Fig.5 Final shear stress versus normal stress in T1S and T2S

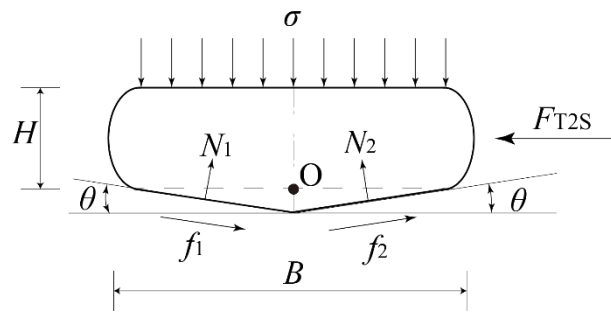


379

380

Fig.6 Angle of insertion versus normal stress in tests T2S and T2P

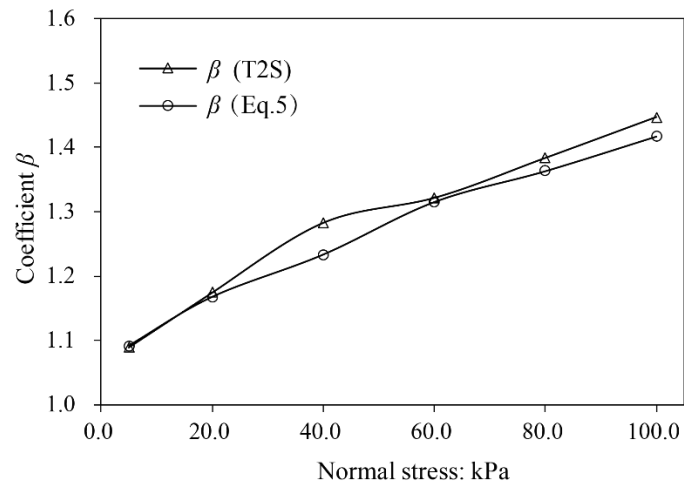
381



382

383

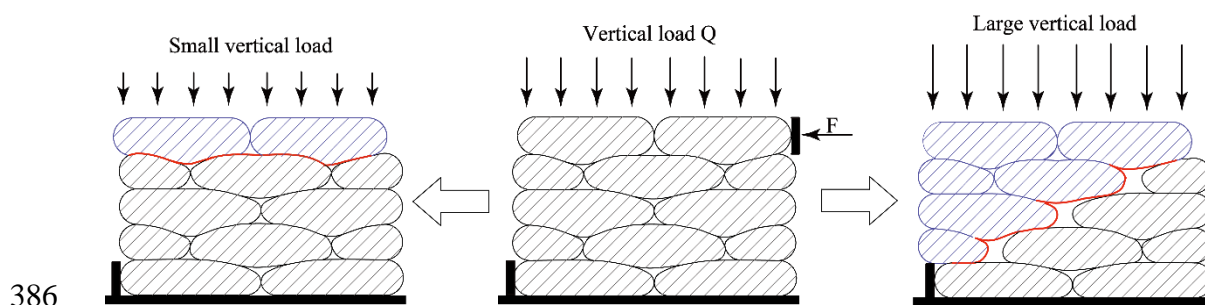
Fig.7 Analysis model for T2S



384

385

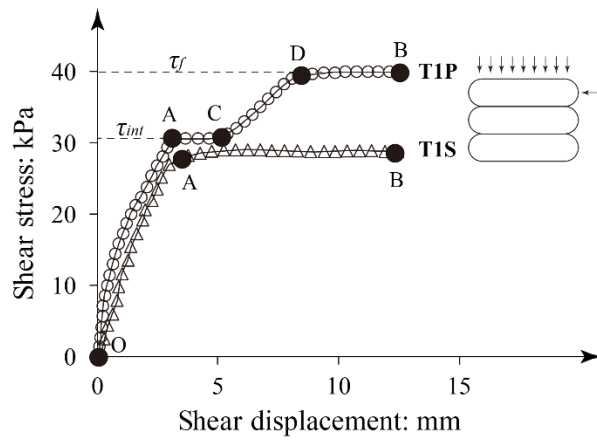
Fig.8 Coefficient  $\beta$  versus normal stress in T2S



386

387

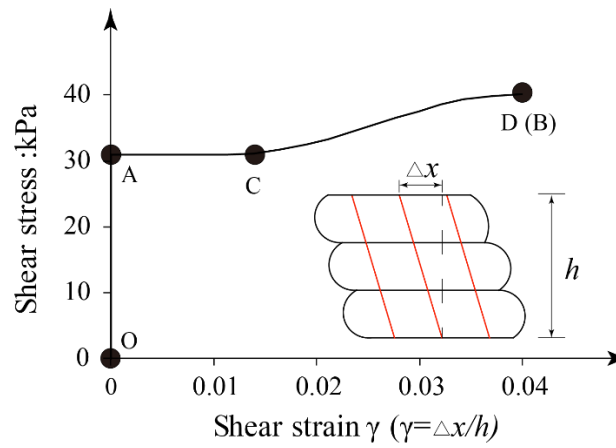
Fig.9 Different sliding surfaces in shear tests on five-layer soilbags



388

389

(a) Shear stress versus shear displacement



390

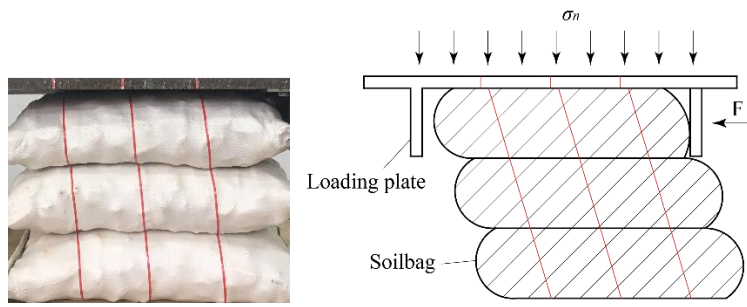
391

(b) Shear stress versus shear strain

392 Fig.10 Shear stress versus shear displacement and shear strain (rotation) in tests T1S

393

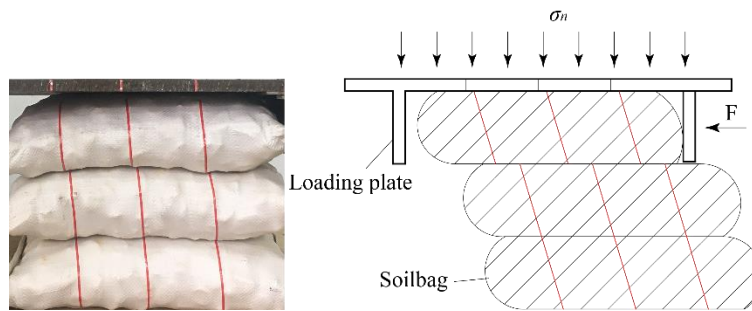
and T1P at  $\sigma_n = 80\text{kPa}$



394

395

(a) Deformation of materials filling the bags in T1P



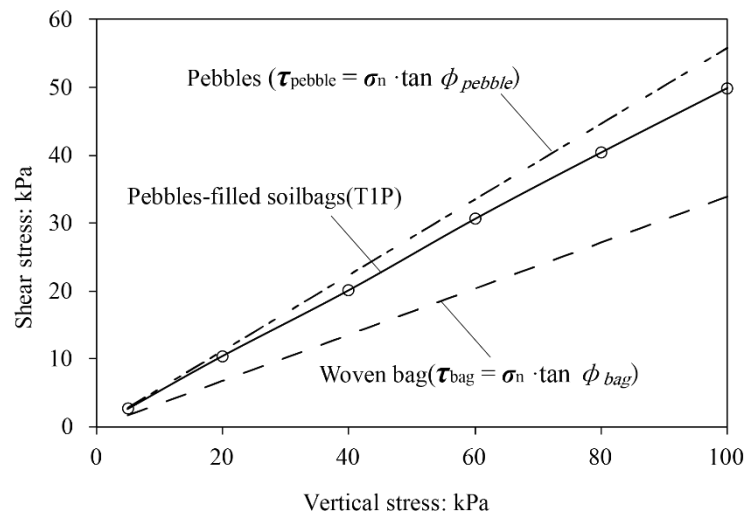
396

397

(b) Interlayer sliding failure

398

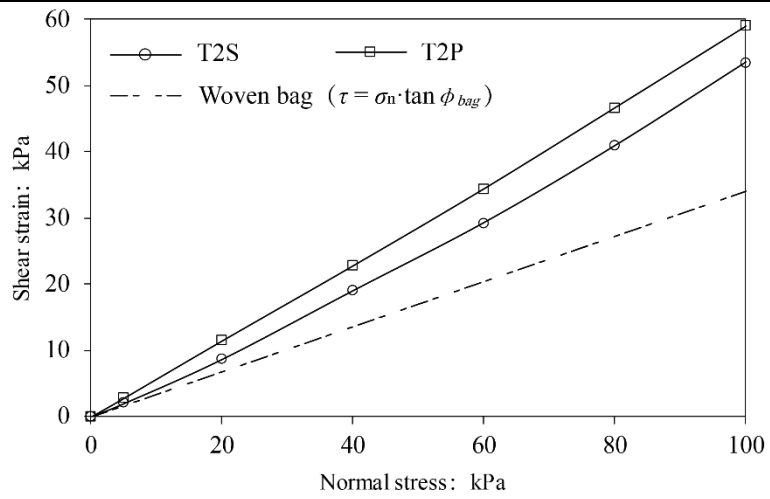
Fig.11 Status of soilbags filled with pebbles during the shearing in T1P



399

400

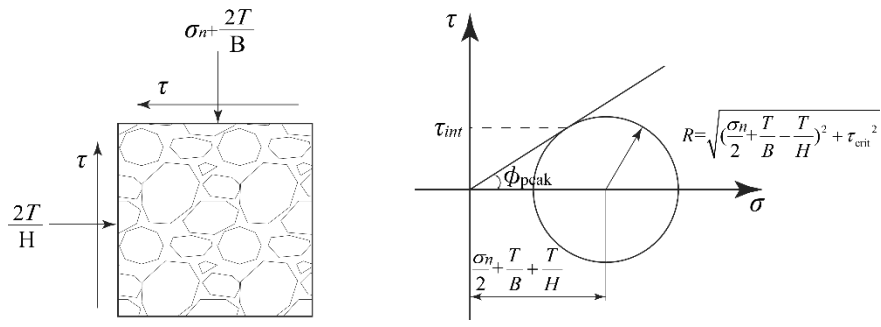
Fig.12 Final shear stress versus normal stress in test T1P



401

402

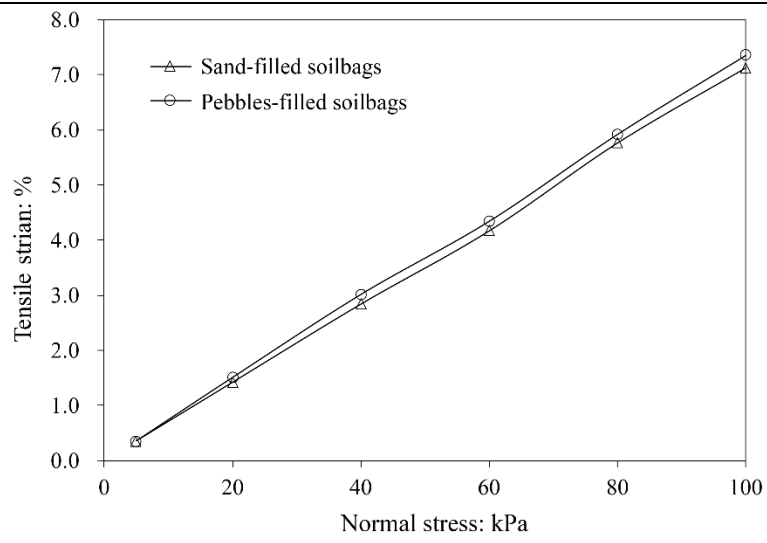
Fig.13 Final shear stress versus normal stress in test T2S and T2P



403

404

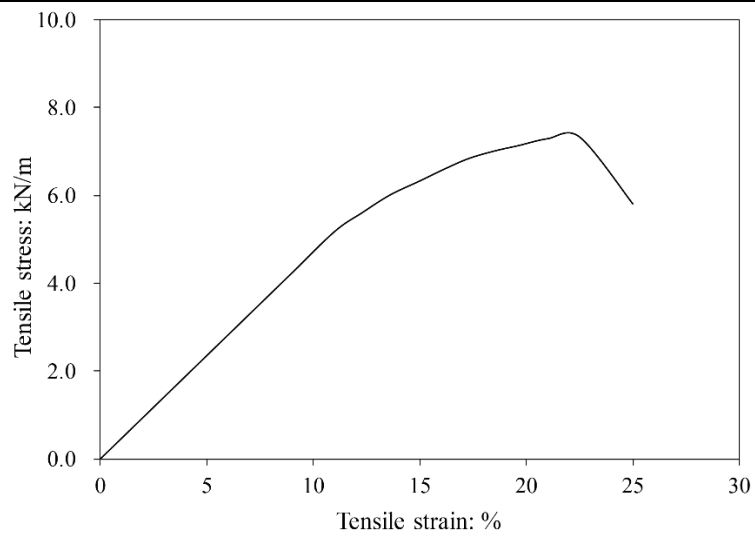
Fig.14 Stress analysis of the element inside the soilbags



405

406

Fig.15 Tensile strain of woven bag versus normal stress applied on soilbag

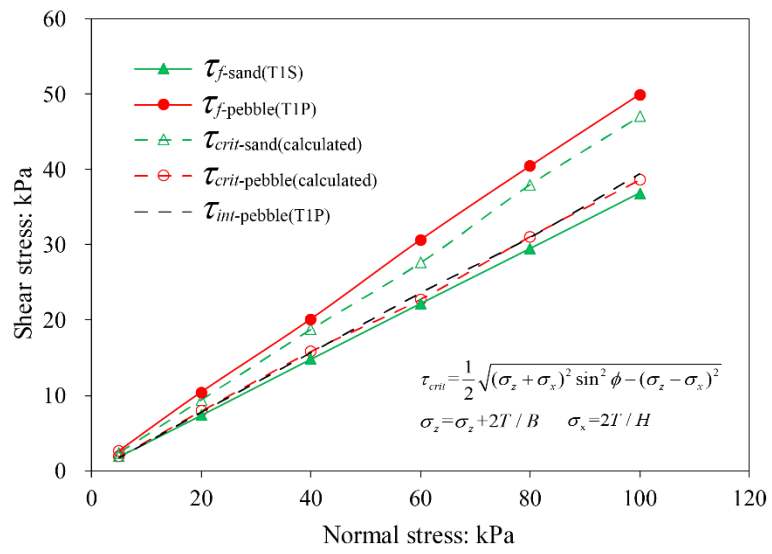


407

408

Fig.16 Tensile behaviour of the woven bags

409



410

411

Fig.17  $\tau_f$  and  $\tau_{crit}$  versus normal stress of soilbags